Received: 7 October 2022 | Accepted: 22 November 2022

DOI: 10.1002/pamm.202200152

Approximate computational model for the local postbuckling of omega-stringer-stiffened composite panels

Jakob C. Schilling[1,*] and **Christian Mittelstedt**[1]

[1] Technical University of Darmstadt, Department of Mechanical Engineering, Institute for Lightweight Construction and Design, Otto-Berndt-Str. 2, 64287 Darmstadt, Germany

Typical thin-walled structures are found in applications like aircraft, spacecraft and marine vessels. For this type of structure, stability behaviour is crucial. The better this behaviour is understood, the better the full lightweight potential can be exploited. For composite structures especially, new fast analysis tools for preliminary design are required to address this issue. Therefore, the local postbuckling of omega-stringer-stiffened composite panels is the subject of a new computational model. The analysis method is computationally highly efficient because it is based on a closed-form analytical approach. The explicit solution is derived based on the principle of the minimum of the total elastic potential. Furthermore, the solution assumes that the initial eigenform does not substantially change in the early postbuckling regime. In this way, the plates of the skin and stringer can be included explicitly in the analysis. Compared to finite element analysis and a closed-form computational model found in the literature, the new analysis tool is assessed. The results indicate excellent agreement for panels, where the bay plate is the most critical element of the panel. The new computational model promises to be a highly efficient tool in the preliminary design framework.

1 Introduction

Especially in the context of preliminary design, the computational efficiency of analysis methods is essential. For the exploitation of the full lightweight potential in thin-walled structures typically employed in applications like aircraft, spacecraft, and marine vessels, numerous parameter studies and optimisations are necessary, resulting in a high number of function evaluations for the different aspects investigated in the analysis. One of these aspects is the stability behaviour of thin-walled structures, which is critical in the design.

The present work deals with the stability behaviour of an omega-stringer-stiffened panel made of composite material. It is representative of a panel in a more extensive fuselage section and sketched in Figure 1. In a), the individual plates in the panel assembly are introduced and the loading condition is indicated in b). Therefore, the panel is loaded by a prescribed displacement leading to uniaxial compression in the longitudinal direction. It is important to note that the longitudinal edges of these panels are considered with periodic boundary conditions introducing the influence of sourrounding fuselage sections. Additionally, the panel is considered simply supported along loaded edges for a conservative approximation. Generally, the local buckling and postbuckling behaviour are of interest, which assumes that the individual plates show no deflection along adjacent edges.

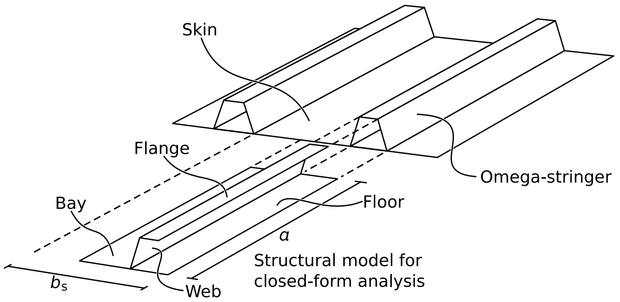

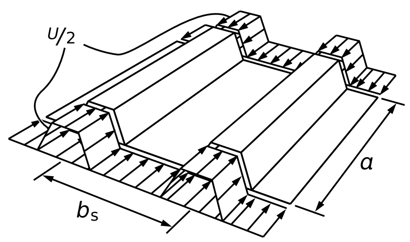

Fig. 1: a) Omega-stringer-stiffened panel with the structural model for the closed-form analysis [1]; b) Loading conditions of the omega-stringer-stiffened panel [1].

This behaviour can be assessed using different computational methods. The highest computational efficiency can be achieved by utilising closed-form analytical approaches compared to finite element, finite strip, and semi-analytical methods. The work of Schilling and Mittelstedt [1] gives an overview of relevant literature and concludes that highly computationally efficient methods are still rare for the analysis of omega-stringer-stiffened panels. The reader is referred to the mentioned reference, as the present paper is its abbreviated version.

* Corresponding author: e-mail jakob.schilling@klub.tu-darmstadt.de, phone +49 6151 16 22027, fax +49 6151 16 21980

The present work introduces a new closed-form analytical approximate solution to the buckling and postbuckling problem of uniaxially compressed omega-stringer-stiffened panels addressing the lack of highly efficient computational methods. The solution is derived based on the principle of the minimum of the total elastic potential. Therefore, the two Marguerre equations are utilised to incorporate the geometric nonlinear behaviour of the deformations and imperfections in the case of the postbuckling analysis. First, a buckling analysis is performed to obtain information about the eigenform, which is the basis for the closed-form analytical postbuckling analysis. The approach to the buckling analysis is based on previous work by the authors concerning the buckling of omega-stringer-stiffened panels [3, 4]. The idealised model for the analysis is presented in Figure 2, with dimensions in a) and the indication of boundary and interface conditions in b). Because of the periodic boundary conditions, the idealised model can be reduced to a four-plate model utilising symmetry conditions. Finally, the results are compared to finite element analyses and the implementation of the model by Vescovini and Bisagni [2] that assumes a single plate reinforced by elastic restraints along the longitudinal edges.

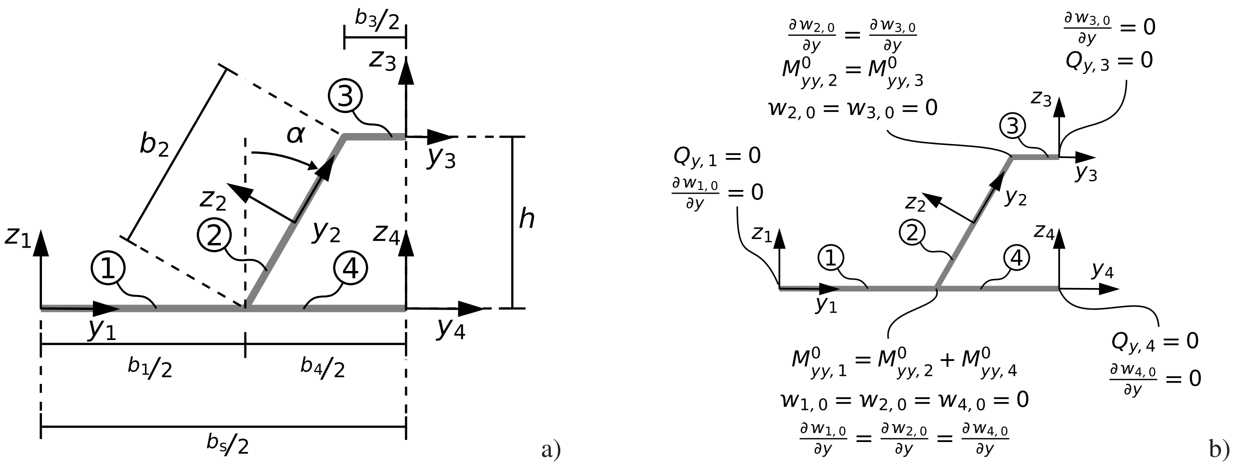

Fig. 2: Idealized model of the omega-stringer-stiffened panel used for the derivation of the buckling and postbuckling analysis: a) dimensions, b) boundary conditions.

2 Methods

2.1 Introduction

As mentioned in the introduction, the governing equations are based on the two Marguerre-type equations. The first is the equilibrium equation given in Eq. (1). Therein, D_{ij} are the bending stiffnesses according to the classical laminated plate theory (CLPT). The deflection w_0 is the deflection of the plate considered and w_i is the initial imperfection in the form of a deflection. In order to achieve the formulation using only two partial differential equations, the Airy stress function ψ is introduced.

$$D_{11}\,\frac{\partial^4 w_0}{\partial x^4} + D_{22}\,\frac{\partial^4 w_0}{\partial y^4} + (2\,D_{12} + 4\,D_{66})\,\frac{\partial^4 w_0}{\partial y^2 \partial x^2} - \left(\frac{\partial^2 w_0}{\partial x^2} + \frac{\partial^2 w_i}{\partial x^2}\right)\frac{\partial^2 \psi}{\partial y^2}$$
$$+\,2\left(\frac{\partial^2 w_0}{\partial y \partial x} + \frac{\partial^2 w_i}{\partial y \partial x}\right)\frac{\partial^2 \psi}{\partial x \partial y} - \left(\frac{\partial^2 w_0}{\partial y^2} + \frac{\partial^2 w_i}{\partial y^2}\right)\frac{\partial^2 \psi}{\partial x^2} = 0 \tag{1}$$

The second is the compatibility equation making sure that the in-plane strains due to bending and stretching are compatible (Eq. (2)). Here, the membrane stiffnesses A_{ij} according to the CLPT are introduced.

$$\bar{A}_{22}\,\frac{\partial^4 \psi}{\partial x^4} + \left(\bar{A}_{66} + 2\,\bar{A}_{12}\right)\frac{\partial^4 \psi}{\partial x^2 \partial y^2} + \bar{A}_{11}\,\frac{\partial^4 \psi}{\partial y^4} = \left(\frac{\partial^2 w_0}{\partial x \partial y}\right)^2 - \frac{\partial^2 w_0}{\partial x^2}\frac{\partial^2 w_0}{\partial y^2} - \frac{\partial^2 w_0}{\partial x^2}\frac{\partial^2 w_\mathrm{i}}{\partial y^2}$$
$$+\,2\,\frac{\partial^2 w_0}{\partial x \partial y}\frac{\partial^2 w_\mathrm{i}}{\partial x \partial y} - \frac{\partial^2 w_\mathrm{i}}{\partial x^2}\frac{\partial^2 w_0}{\partial y^2} \tag{2}$$

where

$$\bar{A}_{11} = \frac{A_{22}}{A_{11}A_{22} - A_{12}^2} \qquad \bar{A}_{22} = \frac{A_{11}}{A_{11}A_{22} - A_{12}^2} \qquad \bar{A}_{12} = \frac{A_{12}}{A_{12}^2 - A_{11}A_{22}} \qquad \bar{A}_{66} = \frac{1}{A_{66}}$$

Both equations are formulated based on von Kármán strains. Detailed descriptions of the strains, constitutive relations and the governing equations can be found in various textbooks like the textbooks by Mittelstedt and Becker [5], Reddy [6], and

Jones [7]. The present computational model is only derived for a specific type of composite material. The analysis approach enables to analyse omega-stringer-stiffened panels made of symmetric cross-ply laminates.

The derivation of the closed-form analytical solution begins with selecting suitable buckling shape functions that can reproduce the deformation of the omega-stringer-stiffened panel in case of buckling. In the present, the deflection of each sub-plate k, numbered according to the idealized model in Figure 2, is expressed by Equation (3). The variables A_0 and B_0 are unknown variational constants equivalent to Ritz-constants that are determined in the course of the analysis by the principle of the minimum of the total elastic potential. The initial imperfections are assumed to be of the same form and thus also based on the polynomial functions $w_{A,\,k}$ and $w_{B,\,k}$. Here, the variables A_i and B_i are the amplitudes of the assumed imperfections.

$$w_{k,\,0} = A_0\, w_{A,\,k}\,(x,\, y_k) + B_0\, w_{B,\,k}\,(x,\, y_k) \tag{3}$$

$$w_{k,\,\mathrm{i}} = A_\mathrm{i}\, w_{A,\,k}\,(x,\, y_k) + B_\mathrm{i}\, w_{B,\,k}\,(x,\, y_k) \tag{4}$$

The polynomial functions $w_{A,\,k}$ and $w_{B,\,k}$ are presented in Equations (5) and (6). To achieve high-quality results using the approximate computational model, the two polynomial functions must fulfil the boundary and interface conditions presented in Figure 2 b). Therefore, the cofactors $c_{Ai,\,k}$ and $c_{Bi,\,k}$ are determined based on the boundary and interface conditions.

$$w_{A,\,k} = \sin\left(\frac{\pi\, m\, x}{a}\right)\left(c_{A0,\,k}\,\frac{{y_k}^4}{{b_k}^4} + c_{A1,\,k}\,\frac{{y_k}^3}{{b_k}^3} + c_{A2,\,k}\,\frac{{y_k}^2}{{b_k}^2} + c_{A3,\,k}\,\frac{y_k}{b_k} + c_{A4,\,k}\right) \tag{5}$$

$$w_{B,\,k} = \sin\left(\frac{\pi\, m\, x}{a}\right)\left(c_{B0,\,k}\,\frac{{y_k}^4}{{b_k}^4} + c_{B1,\,k}\,\frac{{y_k}^3}{{b_k}^3} + c_{B2,\,k}\,\frac{{y_k}^2}{{b_k}^2} + c_{B3,\,k}\,\frac{y_k}{b_k} + c_{B4,\,k}\right) \tag{6}$$

Only the terms for $i = 0$ corresponding to the variational constants A_0 and B_0 are prescribed based on the definition given in Equation (7).

$$c_{A0,\,k} = [1,\, 0,\, 0,\, 0] \qquad\qquad c_{B0,\,k} = [0,\, 1,\, 0,\, 0] \tag{7}$$

With the defined deflection $w_{k,\,0}$ and imperfection $w_{k,\,\mathrm{i}}$, the next step is the definition of the Airy stress function before the total elastic potential is computed.

2.2 Airy stress function

The Airy stress function is generally defined to fulfil the relations given in Equation (8), so that the resultant forces $N^0_{xx,\,k}$, $N^0_{yy,\,k}$, and $N^0_{xy,\,k}$ are expressed depending on the Airy stress function ψ_k.

$$N^0_{xx,\,k} = \frac{\partial^2 \psi_k\,(x,\, y_k)}{\partial y_k^2} \qquad N^0_{yy,\,k} = \frac{\partial^2 \psi_k\,(x,\, y_k)}{\partial x^2} \qquad N^0_{xy,\,k} = -\frac{\partial^2 \psi_k\,(x,\, y_k)}{\partial y_k \partial x} \tag{8}$$

In the present approach, the solution for the Airy stress function is built of three separate parts as given in Equation (9). It consists of the particular solution $\psi_{\mathrm{p},\,k}$ and two homogeneous solutions $\psi_{\mathrm{h},\,1,\,k}$ and $\psi_{\mathrm{h},\,2,\,k}$. The solution is obtained by ensuring that the compatibility equation given in Equation (2) is fulfilled.

$$\psi_k = \psi_{\mathrm{h},\,1,\,k} + \psi_{\mathrm{h},\,2,\,k} + \psi_{\mathrm{p},\,k} \tag{9}$$

For brevity, the reader is referred to Ref. [1] for the derivation of the particular solution, ensuring that the left-hand and right-hand sides of the mentioned partial differential equation are compatible. Also, the detailed derivation of the homogeneous solutions is presented in Ref. [1] and omitted here. The homogeneous solutions can be finally obtained in the following form (Eq. (10) and (11)). Therein, the cofactors $C_{1,\,k}$, $C_{2,\,k}$, $C_{3,\,k}$, $C_{4,\,k}$, $C_{5,\,k}$, and $C_{u,\,k}$ are determined by utilizing the in-plane boundary conditions of the individual plates.

$$\begin{aligned}\psi_{\mathrm{h},\,1,\,k}\,(x, y_k) = &\cos\left(\frac{2\,\pi\, m\, x}{a}\right)\,(C_{1,\,k}\cosh\left(\lambda_{1,\,k}\, y_k\right) + C_{2,\,k}\sinh\left(\lambda_{1,\,k}\, y_k\right) + C_{3,\,k}\cosh\left(\lambda_{2,\,k}\, y_k\right)\\ &+ C_{4,\,k}\sinh\left(\lambda_{2,\,k}\, y_k\right))\end{aligned} \tag{10}$$

$$\psi_{\mathrm{h},2,\,k}\,(x, y_k) = C_{5,\,k}\,\frac{y_k^2}{b_k^2} + C_{u,\,k}\,\frac{y_k^3}{b_k^3} \tag{11}$$

Consequently, the two homogeneous solutions are necessary to include the in-plane boundary conditions in the analysis. The in-plane boundary conditions for the longitudinal edges of the sub-plates are given in Equations (12) and (13). They require the vanishing of shear force resultants and that the edges remain straight.

$$N^0_{xy,\,k}\left(x, y_k = \pm\,\frac{b_k}{2}\right) = 0 \tag{12}$$

$$v_k\left(x,\, y_k = \pm\,\frac{b_k}{2}\right) = \text{const.} \tag{13}$$

With these conditions the cofactors $C_{1,\,k}$, $C_{2,\,k}$, $C_{3,\,k}$, and $C_{4,\,k}$ are determined. The remaining cofactors $C_{5,\,k}$ and $C_{u,\,k}$ are obtained by evaluating the prescribed displacement along the transverse edges of the sub-plates. Here it is required that the displacement u_k is equal to the prescribed displacement U and additionally that the displacement is uniform, meaning independent of the transverse coordinate y_k.

2.3 Total elastic potential

The total elastic potential is computed with the definition of the deflection, imperfection and the Airy stress function. The formulation for the contributions of the individual sub-plates is expressed in Equations (14) and (15), which are the contributions due to the membrane $\Pi_{\mathrm{m},\,k}$ and the bending $\Pi_{\mathrm{b},\,k}$ behaviour of the sub-plates.

$$\Pi_{\mathrm{m},\,k} = \frac{1}{2}\int_0^a \int_{-\frac{b_k}{2}}^{\frac{b_k}{2}} \left\{ \bar{A}_{22}\left(\frac{\partial^2 \psi_k}{\partial x^2}\right)^2 + \bar{A}_{66}\left(\frac{\partial^2 \psi_k}{\partial y_k \partial x}\right)^2 + \bar{A}_{11}\left(\frac{\partial^2 \psi_k}{\partial {y_k}^2}\right)^2 + 2\,\bar{A}_{12}\,\frac{\partial^2 \psi_k}{\partial x^2}\,\frac{\partial^2 \psi_k}{\partial {y_k}^2} \right\} \mathrm{d}y\mathrm{d}x \quad (14)$$

$$\Pi_{\mathrm{b},\,k} = \frac{1}{2}\int_0^a \int_{-\frac{b_k}{2}}^{\frac{b_k}{2}} \left\{ D_{11}\left(\frac{\partial^2 w_0}{\partial x^2}\right)^2 + 4\,D_{66}\left(\frac{\partial w_0}{\partial y_k \partial x}\right)^2 + D_{22}\left(\frac{\partial^2 w_0}{\partial y_k^2}\right)^2 + 2\,D_{12}\,\frac{\partial^2 w_0}{\partial x^2}\,\frac{\partial^2 w_0}{\partial y_k^2} \right\} \mathrm{d}y\mathrm{d}x \quad (15)$$

The individual contributions are then summed to obtain the total elastic potential $\Pi\,(A_0,\,B_0)$ that is now only depending on the two variational constants. With this, the solution of the linear buckling problem and then the postbuckling problem is obtained.

2.4 Buckling analysis

In order to obtain the critical eigenform of the linear buckling problem, the total elastic potential is first simplified. Therefore, the constants $A_i,\ {A_0}^4,\ {A_0}^3,\ B_i,\ {B_0}^4,\ {B_0}^3,\ {A_0}^2\,{B_0}^2$ are omitted.

It is now possible to utilise the principle of the minimum of the total elastic potential to perform the eigenvalue analysis. As a result, the critical displacement is obtained in an explicit, closed-form analytical fashion. Thus, the eigenform of the buckled panel can be determined.

$$U_{\mathrm{cr}} = -\,\frac{\Psi_2 \pm \sqrt{-4\,\Psi_1\,\Psi_3 + {\Psi_2}^2}}{2\,\Psi_1} \qquad \text{where} \qquad \begin{aligned} \Psi_1 &= 4\,K_5\,K_{12} - {K_9}^2 \\ \Psi_2 &= 4\,K_5\,K_{13} + 4\,K_6\,K_{12} - 2\,K_9\,K_{10} \\ \Psi_3 &= 4\,K_6\,K_{13} - {K_{10}}^2 \end{aligned} \quad (16)$$

For the variables K_q for $q = 1,\,2,\,3,\ldots,\,14$ the expressions are presented in Ref. [1] and not reprinted here for brevity.

From the solution of the linear eigenvalue problem the ratio $\delta_{B/A}$ between the amplitudes B_0 and A_0 is obtained and an important input for the postbuckling analysis (Eq. (17)). Also, the critical half-wave number m is obtained. Thus, the eigenform is obtained qualitatively.

$$\delta_{B/A} = \frac{B_0}{A_0} = -\frac{2\,K_5\,U_{\mathrm{cr}} + 2\,K_6}{K_9\,U_{\mathrm{cr}} + K_{10}} \quad (17)$$

With the obtained ration the constants B_0 and B_{i} can be expressed as follows in Equations (18).

$$B_0 = \delta_{B/A}\,A_0 \qquad\qquad B_{\mathrm{i}} = \delta_{B/A}\,A_{\mathrm{i}} \quad (18)$$

2.5 Postbuckling analysis

Using the eigenform of the linear buckling analysis, the total elastic potential introduced in Section 2.3 is simplified. The relations of Equations (18) are introduced and the constants B_0 and B_{i} substituted. Therefore, the total elastic potential for the postbuckling problem only depends on the variational constant A_0. If the principle of the minimum of the total elastic potential is used, only one Ritz-equation is obtained. It is presented in Equation (19).

$$\frac{\partial \Pi}{\partial A_0} = A_0\,L_4 + L_1\,\left({A_0}^3 + 3\,{A_0}^2\,A_i\right) + L_3\,\left(A_0\,U + A_i\,U\right) + A_0\,{A_i}^2\,L_2 = 0 \quad (19)$$

where

$$L_1 = 4\,K_{11}\,\delta_{B/A} + 4\,K_7\,{\delta_{B/A}}^3 + 4\,K_3\,{\delta_{B/A}}^2 + 4\,K_2\,\delta_{B/A} + 4\,K_1$$

$$L_2 = 8\,K_{11}\,{\delta_{B/A}}^4 + 8\,K_7\,{\delta_{B/A}}^3 + 4\,K_4\,{\delta_{B/A}}^2 + 2\,K_8\,{\delta_{B/A}}^2 + 8\,K_2\,\delta_{B/A} + 8\,K_1$$

$$L_3 = 2\,K_{12}\,{\delta_{B/A}}^2 + 2\,K_9\,\delta_{B/A} + 2\,K_5 \qquad L_4 = 2\,K_{13}\,{\delta_{B/A}}^2 + 2\,K_{10}\,\delta_{B/A} + 2\,K_6$$

The solution for the variational constant A_0, which is now equivalent to a postbuckling amplitude, scales the deformation initially obtained as the eigenform in the linear buckling analysis. Note that only the real root of the three solutions gives plausible results. Therefore, only the relevant root is reprinted here in Equation (20).

$$A_{0,1} = -(\beta_2 - \beta_1) - \frac{O_1}{3} \tag{20}$$

where

$$\beta_1 = \left(\sqrt{\left(\frac{{O_1}^3}{27} - \frac{O_1\, O_2}{6} + \frac{O_3}{2} \right)^2 + \left(-\frac{{O_1}^2}{9} + \frac{O_2}{3} \right)^3} - \frac{{O_1}^3}{27} - \frac{O_3}{2} + \frac{O_1\, O_2}{6} \right)^{1/3}$$

$$\beta_2 = -\frac{1}{\beta_1} \left(\frac{{O_1}^2}{9} + \frac{O_2}{3} \right) \qquad O_1 = 3\, A_i \qquad O_2 = \frac{L_4}{L_1} + \frac{L_3\, U}{L_1} + \frac{{A_i}^2\, L_2}{L_1} \qquad O_3 = \frac{A_i\, L_3\, U}{L_1}$$

The postbuckling amplitude A_0 enables a quantitative description of the local postbuckling behaviour of omega-stringer-stiffened panels in the early postbuckling range. This includes the deformation but also stresses and resultant forces and moments, as well as postbuckling parameters such as the effective width. The closed-form analytical method is limited to the proximity of the initial buckling because no mode changes are detected. This is, however, well within the requirements of preliminary design. The results presented in the next section show the capabilities of the closed-form analytical method.

3 Results and discussion

The results obtained with the computational model introduced in the previous section are evaluated compared to finite element analyses and an implementation of the model described by Vescovini and Bisagni [2]. The length of the investigated panel a is $600\,\mathrm{mm}$, the spacing b_s is $200\,\mathrm{mm}$, the angle α is $25°$, and the ratio b_4/h is 1.833. For the results presented in the following, a symmetric cross-ply laminate is used for all four sub-plates. The stacking sequence is $[0°/90°/0°/90°]_\mathrm{s}$, with a ply thickness of $0.184\,\mathrm{mm}$. The material properties are $E_1 = 157\,000\,\mathrm{MPa}$, $E_2 = 8500\,\mathrm{MPa}$, $G_{12} = 4200\,\mathrm{MPa}$ and $\nu_{12} = 0.35$.

Since the postbuckling analysis depends on the eigenform of the linear buckling analysis, it is interesting to look at the results for the critical displacement U_cr. This leads to a first impression of the quality of the present computational model. If it performs with high accuracy for buckling, it can be assumed that high-quality results are obtained for the early postbuckling range. In Figure 3 a), the critical displacement is plotted versus the ratio $b_4/(b_1+b_4)$, which scales the size of the stringer keeping the dimensions as introduced in the previous paragraph. The results show that for typical stringer-stiffened panels, where the bay plate is larger in width than the floor plate of the stringer, the present and the referenced closed-form analytical models achieve very good agreement. The agreement of the present method is hereby superior to the simpler model of Vescovini and Bisagni [2] denoted as $\mathrm{CF_{VB12}}$. In the following results, the ratio $b_4/(b_1+b_4) = 0.25$ is considered representative for a

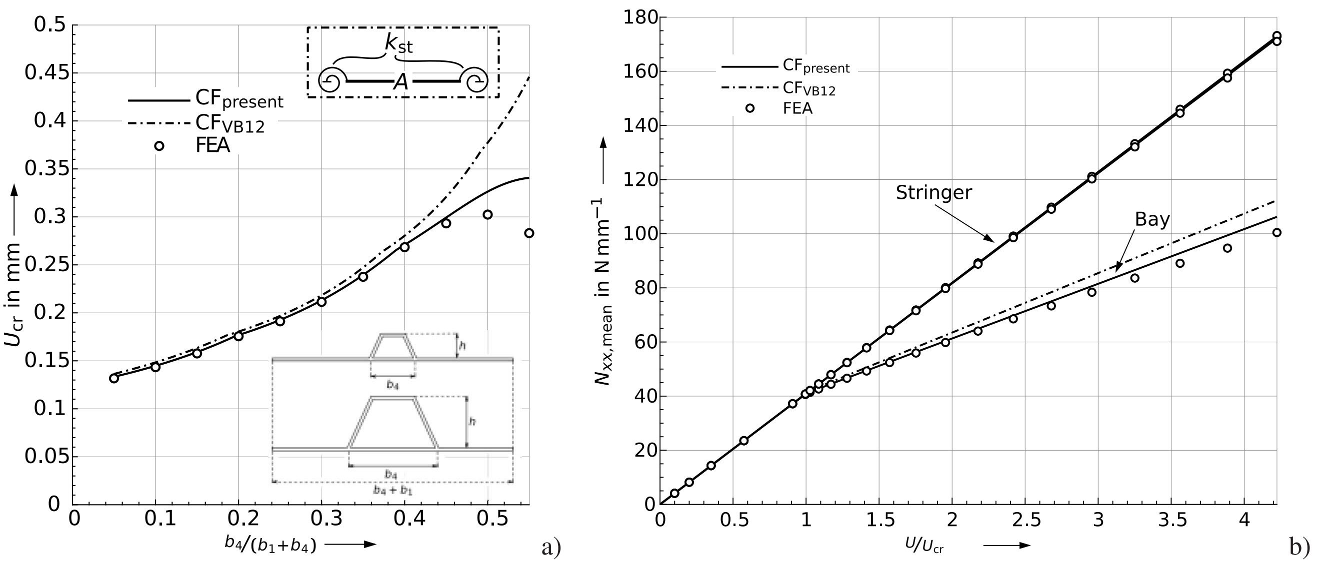

Fig. 3: Results obtained by the present model $\mathrm{CF_{present}}$, the model of Ref. [2] $\mathrm{CF_{VB12}}$ and the FEA: a) Critical displacement U_cr for different ratios $b_4/(b_1+b_4)$ [1]; b) Force-displacement relationship for all four sub-plates for the ratio $b_4/(b_1+b_4) = 0.25$ [1].

typical omega-stringer-stiffened panel. In Figure 3 b) the load-displacement curves are plotted. They include the results for the four sub-plates obtained by the FEA and the present model $CF_{present}$. The model CF_{VB12} can only predict the postbuckling behaviour of a single plate at once. Consequently, the results for the bay plate show suitable agreement. As before, the present model performs with a very good agreement and reproduces the typical postbuckling behaviour of a stiffened panel, where the stringer continues to carry load even though the bay plate is buckled and shows a loss of stiffness.

This is also reflected in Figure 4 a), where the load distribution for different stages in the postbuckling range is given for all four plates. The load-carrying capability of the stringer plates is only slightly changing, whereas the bay plate is significantly

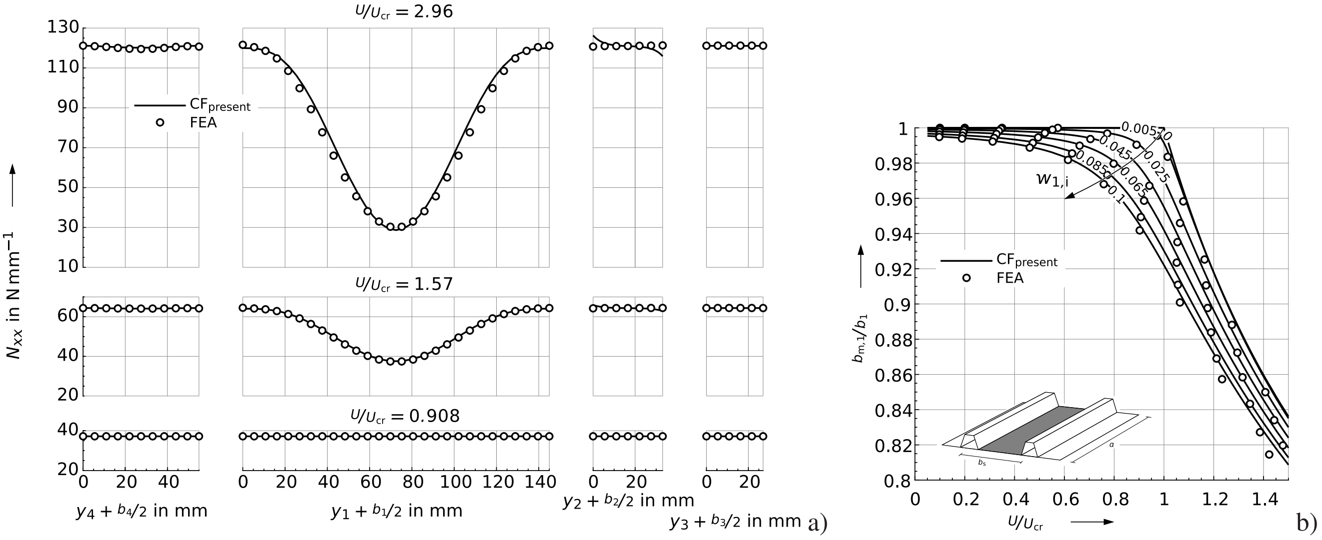

Fig. 4: Results obtained by the present model $CF_{present}$ and the FEA for the ratio $b_4/(b_1+b_4) = 0.25$: a) Load distribution $N_{xx}(y_k)$ for different ratios $b_4/(b_1+b_4)$ [1]; b) Effective width b_{eff} for the bay plate with varied imperfection w_i [1].

weakened with progressing compression. The present model predicts the load distributions with good agreement. In the previously discussed results the imperfection w_i is set to 2×10^{-3} mm. However, in Figure 4 b), the size of the imperfection is varied to show the influence of the imperfection on the effective width for increasing compression of the panel. This influence is only shown for the bay plate, as a significant reduction of the effective width occurs here, corresponding to the previously discussed load distributions within the four sub-plates. Notably, the imperfection's size directly influences the loss of effective width, especially in the early postbuckling range. A loss of effective width can even occur before the critical displacement is reached.

The results showed that the new closed-form analytical model achieves very good agreement in analysing the local stability behaviour of omega-stringer-stiffened panels. However, it is limited to symmetric cross-ply laminates and the early postbuckling range. Mode changes are not detected, as the postbuckling analysis depends on the eigenform of the linear buckling analysis. The analysis approach enables the characterisation of the individual sub-plates of the stiffened panel and is not limited to one plate as alternative models that assume a single plate with elastic restraints. For a more detailed derivation and discussion of results, the reader is referred to Ref. [1]. The present computational model offers a novel, highly efficient tool for the preliminary design of this type of thin-walled structure.

Acknowledgements The financial support of the German Research Foundation DFG [project numbers 399128978 and 426146527] is acknowledged with gratitude. Open access funding enabled and organized by Projekt DEAL.

References

[1] J.C. Schilling and C. Mittelstedt, Thin-Walled Struct. **181**, 110027 (2022).
[2] R. Vescovini and C. Bisagni, Compos. B. Eng. **43**, 1258–1274 (2012).
[3] J.C. Schilling and C. Mittelstedt, Thin-Walled Struct. **147**, 106534 (2020).
[4] J.C. Schilling and C. Mittelstedt, Int. J. Mech. Sci. **207** 106646 (2021).
[5] C. Mittelstedt and W. Becker, Strukturmechanik ebener Laminate (Studienbereich Mechanik, Darmstadt, 2016).
[6] J.N. Reddy, Mechanics of laminated composite plates and shells: theory and analysis (CRC Press, Boca Raton, 2004).
[7] R.M. Jones, Mechanics of composite materials (Taylor & Francis, Philadelphia, 1999).

